Flight-Level Thermodynamic Instrument Wetting Errors in Hurricanes. Part I: Observations

MATTHEW D. EASTIN

Department of Atmospheric Science, Colorado State University, Fort Collins, Colorado

PETER G. BLACK

Hurricane Research Division, NOAA/AOML Miami, Florida

WILLIAM M. GRAY

Department of Atmospheric Science, Colorado State University, Fort Collins, Colorado

(Manuscript received 1 March 2001, in final form 5 October 2001)

ABSTRACT

Flight-level thermodynamic errors caused by the wetting of temperature and moisture sensors immersed within the airstream are studied using data from 666 radial legs collected in 31 hurricanes at pressure levels ranging from 850 to 500 mb. Concurrent measurements from a modified Barnes radiometer and a Rosemount 102 immersion thermometer are compared to identify regions, called instrument wetting events (IWE), in which Rosemount temperatures are significantly cooler than radiometer-derived temperatures by a specified amount. A total of 420 IWE are identified in the dataset. Roughly 50% of the radial legs contain at least one instrument wetting event. More than 90% of IWE are associated with updrafts containing cloud water and are confined to scales less than 10 km. IWE are also found to be more frequent in eyewalls and intense hurricanes.

Thermodynamic errors within IWE and convective updrafts and downdrafts are summarized as distributions of average temperature, specific humidity, virtual potential temperature, and equivalent potential temperature error. Distributions are skewed toward larger error values at all levels. Median average errors within IWE indicate that the thermodynamic quantities are typically too low by ~1°C, ~1 g kg^{-1}, ~1.5 K, and ~5 K, respectively. The largest errors (>90% of the distribution) are nearly twice the median values. Error magnitudes tend to increase with height, but rarely achieve theoretical predictions. In addition, more than 65% of updrafts and 35% of downdrafts are found to contain significant thermodynamic errors. A correction method used in earlier studies was found to be inadequate at removing the majority of errors, but reduced the errors by ~30%–50% on average.

1. Introduction

Cumulus convection has long been recognized to play a crucial role in hurricane evolution (e.g., Riehl 1954) but has yet to be fully understood. One well-recognized limitation is the inability to collect accurate in situ thermodynamic observations in the convection with instrumented aircraft. Temperature and moisture sensors have historically been mounted to the aircraft exterior and thus immersed directly in the airstream. These ''immersion sensors'' can become wet in clouds and precipitation and experience large ''instrument wetting errors.'' Lenschow and Pennell (1974) and Lawson and Cooper (1990) showed that the temperature measured by a wet thermometer exposed to dynamically heated air can theoretically be underestimated by as much as 5°–7°C at typical aircraft speeds. The wetting of moisture sensors can result in dewpoint errors equivalent to 1°–2°C above saturation (Zipser et al. 1981). Such errors can significantly affect the magnitudes of thermodynamic quantities, such as virtual potential temperature and equivalent potential temperature, used in the evaluation of hurricane convection, structure, and evolution.

a. Background

The aircraft has been the primary platform used to collect in situ thermodynamic data in hurricanes since penetrations began in the 1940s. Simpson (1952) indirectly documented the first evidence of instrument wetting errors. He noted that during passage through the eyewall of Typhoon Marge (1951) an immersion temperature sensor measured a 21.6°C drop as ice accumulated upon the aircraft surfaces. Subsequent hur-

Corresponding author address: Matthew D. Eastin, Department of Atmospheric Science, Colorado State University, Fort Collins, CO 80523.
E-mail: eastin@mpi.atmos.colostate.edu

© 2002 American Meteorological Society

Unauthenticated | Downloaded 02/22/24 05:18 AM UTC

TABLE 1. Notable studies addressing hurricane thermodynamics with flight-level data and their treatment of either local temperature minima within convection or instrument wetting errors. The ZML temperature correction method proposed by Zipser et al. (1981) is described in section 4e. The JL method is described in Jorgensen and LeMone (1989) and is similar to the method used in this paper.

Study	Temperature sensor(s) used	Local temperature minima in convection		
		Observed	Suspected cause(s)	Correction method
Simpson (1952)	Immersion	No	—	—
Jordan (1958a)	Vortex immersion	Yes	Rain evaporation	—
Riehl and Malkus (1961)	Vortex immersion	Yes	Instrument wetting	Adjusted to fit sounding
LaSeur and Hawkins (1963)	Vortex immersion	Yes	Instrument wetting Rain evaporation	—
Colon (1964)	Vortex immersion	Yes	Rain evaporation Instrument lag Adiabatic cooling of inflow	—
Gentry (1964)	Vortex immersion	Yes	Rain evaporation	—
Gray (1965)	Vortex immersion	Yes	Instrument wetting	—
Sheets (1967a, b, 1968)	Vortex immersion	Yes	Instrument wetting Rain evaporation	—
Hawkins and Rubsam (1968)	Vortex immersion	Yes	Instrument wetting	—
Shea and Gray (1973)	Vortex immersion	No	—	—
Gray and Shea (1973)	Vortex immersion	No	—	—
Hawkins and Imbembo (1976)	Vortex immersion	No	—	—
	Aircraft and instrumentation change			
Riehl (1981)	Rosemount immersion	No	—	—
Barnes et al. (1983)	Rosemount immersion	Yes	Instrument wetting	ZML method
Jorgensen (1984a,b)	Rosemount immersion	Yes	Instrument wetting	ZML method
Frank (1984)	Rosemount immersion	Yes	Instrument wetting	—
Barnes and Stossmeister (1986)	Rosemount immersion	Yes	Instrument wetting	ZML method
Powell (1987)	Rosemount immersion	Yes	Instrument wetting	—
Powell (1990)	Rosemount immersion	Yes	Instrument wetting	ZML method
Barnes et al. (1991)	Radiometer and Rosemount immersion	Yes	Instrument wetting	JL method
Ryan et al. (1992)	Radiometer and Rosemount immersion	Yes	Instrument wetting	JL method
Black et al. (1994)	Radiometer and Rosemount immersion	Yes	Instrument wetting	Used warmest temp. from immersion and radiometric sensors
Black and Holland (1995)	Rosemount immersion	Yes	Instrument wetting	—
Barnes and Powell (1995)	Radiometer and Rosemount immersion	Yes	Instrument wetting	JL method

ricane studies (see Table 1) noted that local temperature minima on the order of 1°–3°C (and supersaturated conditions) were frequently observed by vortex immersion thermometers (Hilleary and Christensen 1957) during passage through clouds and precipitation. The local minima were attributed not only to instrument wetting but also to evaporation of rain, adiabatic cooling of inward spiraling air, and instrument time lags. Few adjustments were made to these apparent erroneous temperatures since no systematic correction method was established (Hawkins and Rubsam 1968). However, supersaturated dewpoints were typically adjusted to saturation. The data from these early aircraft penetrations were primarily used to piece together the three-dimensional inner-core (defined here as within 150 km of storm center) structure, and convective scale thermodynamic errors were not believed to produce a statistically significant effect (Shea and Gray 1973). However, the few early studies that focused on the convective scales (Gentry 1964; Gray 1965) could not determine thermodynamic quantities with confidence due to suspected instrument wetting errors.

In the mid-1970s the acquisition of the two National Oceanic and Atmospheric Administration (NOAA) WP-3D research aircraft with improved instrumentation, navigation equipment, and data collection resolution shifted the emphasis of hurricane research toward mesoscale and convective scale structure (e.g., Barnes et al. 1983). The primary thermodynamic instruments became a Rosemount 102 total temperature sensor and a General Eastern chilled-mirror hygrometer. Both immersion instruments were designed to inertially separate water particles from the air prior to measurement, and thus, minimize instrument wetting errors. However, local temperature minima and supersaturated dewpoints continued to be concurrently observed in convection.

Unauthenticated | Downloaded 02/22/24 05:18 AM UTC

TABLE 2. Performance specifications of thermodynamic instrumentation used in this study (Jorgensen 1984a).

Instrument	Parameter	Data precision	Absolute accuracy	Time constant
Rosemount 102CH2AF (de-iced) total temperature probe	Temperature	0.03°C	±0.2°C	1–2 s
Barnes PRT-5 radiometer	Temperature	0.01°C	±0.5°C	<1 s
General Eastern 1011B hygrometer	Dewpoint	0.03°C	±0.4°C (dewpoint) ±0.6°C (frost point)	5–20 s

The supersaturated dewpoints could be adjusted to saturation, but analytic temperature corrections were unreliable since the error was a function of how much of the sensor was wet (Lenschow and Pennell 1974). Again, studies addressing hurricane convection (e.g., Jorgensen et al. 1985) could not deduce thermodynamic properties of updrafts and downdrafts due to instrument wetting errors.

Zipser et al. (1981) estimated that maximum temperature and dewpoint errors induced by wetting were ~1.5°C. In order to study the mesoscale structure of a convective band they proposed a simple method to further *reduce* these errors: if the dewpoint exceeded the temperature, the temperature was adjusted to the average of the two measurements and saturation was assumed. This method (hereafter referred to as the ZML method) was used in several subsequent mesoscale studies of hurricanes (Barnes et al. 1983; Jorgensen 1984b; Barnes and Stossmeister 1986; Powell 1990), but its ability to effectively *remove* instrument wetting errors on either the mesoscale or convective scale is unknown.

In recent years short-path infrared radiometers were installed on the research aircraft. Short-path radiometers provide an indirect measurement of flight-level air temperature without placing a sensor directly in the airstream. Therefore, radiometers provide more accurate temperature measurements in and near convection without the adverse effects of sensor wetting. Lawson and Cooper (1990) noted, however, that radiometers can suffer from time-dependent offsets and calibration problems in flight. Jorgensen and LeMone (1989) found that upon removal of any offsets, the radiometric temperature estimates could be used to analyze thermodynamic quantities in convective updrafts and downdrafts with confidence. Despite the radiometer's advantage, only a few studies of hurricane convective and mesoscale structure (Barnes et al. 1991; Black et al. 1994; Barnes and Powell 1995) have utilized radiometric temperature data.

b. Goals

The availability of a radiometer that provides an independent and more accurate temperature measurement within convection affords the opportunity to evaluate the Rosemount sensor and the ZML correction method within the hurricane inner core. Therefore, the objective of this study is to utilize concurrent measurements from a modified Barnes radiometer and a Rosemount 102 total temperature sensor to develop statistics of instrument wetting errors within hurricane inner-core flight-level data. Specific questions to be answered include

1) How frequent are significant instrument wetting errors observed in the hurricane inner core?
2) What are typical wetting error magnitudes?
3) How frequent, and of what magnitude, are instrument wetting errors in convective updrafts and downdrafts?
4) How effective is the ZML correction method at removing the errors?

This paper, which is Part I of a two-paper series, reviews the flight-level thermodynamic instrumentation and their potential sources of errors, presents summary statistics of instrument wetting errors, and evaluates the ZML correction method. In Part II, scientific implications of error removal are discussed in regards to mean eyewall radial structure, buoyancy within rainband vertical motions, and vertical energy fluxes near the top of the inflow layer.

2. Instrumentation and review of potential errors in convection

The basic flight-level instrumentation and navigation systems on the two NOAA WP-3D aircraft are identical and have been described by Jorgensen (1984a). This section discusses the basic design of the three thermodynamic sensors used in this study and the potential errors of each instrument within convection. Use of the term instrument wetting error is also addressed. Performance specifications of each instrument are listed in Table 2.

a. Radiometric thermometer

The radiometer used in this study is a modified Barnes PRT-5 that utilizes the 15-μm spectral band (a CO_2 absorption line). The instrument measures the total radiance emitted by the ambient air within a horizontally directed 2° conical volume and compares this radiance to the total radiance emitted by a temperature-controlled

Unauthenticated | Downloaded 02/22/24 05:18 AM UTC

blackbody. The flight-level air temperature is then determined by inverting the Planck function and assuming the total radiance observed in the conical volume is proportional to a weighted average of the temperature in that volume (Albrecht et al. 1979).

The indirect measurement of flight-level air temperature eliminates instrument wetting errors, however, temperatures obtained by radiometers still have two potential sources of error. The first arises from water being a strong absorber (and emitter) within the 15-μm band. When water particles are present within the sampled volume the measured temperature will be a weighted combination of the radiances emitted by the water and the air. Thus, the measured temperature will be in error if the water particles are at a different temperature than the ambient air. The temperature of growing cloud drops and ice crystals are typically less than 0.1°C warmer than the local air since supersaturations are believed to be less than 1% in even the strongest updrafts (Pruppacher and Klett 1997). However, the temperature of evaporating hydrometeors approach the wet-bulb temperature of the ambient air. Therefore, in subsaturated regions containing hydrometeors, the measured temperature may be in error by as much as 1°–2°C depending upon liquid water contents and ambient relative humidity.

A second source of error arises from the aircraft roll and the pathlength of the observed radiance. A small error results during periods of roll since the measured temperature is a weighted average over the vertical temperature gradient. Albrecht et al. (1979), using a similar radiometer, showed that in clear air the pathlength of the observed radiance was ~200 m from the aircraft, but in a stratus cloud with a liquid water content of only 0.2 g m^{-3} the pathlength was reduced to 33 m from the aircraft. Therefore, errors induced by aircraft roll will be insignificant in clouds due to the shortened pathlength. However, significant errors may be introduced during periods of high roll in clear air. For example, during a 10° roll in clear air a fraction of the total observed radiance may originate up to 50 m vertically offset from flight level. Assuming a lapse rate of 7.0°C km^{-1} temperature errors up to 0.5°C can result.

b. Immersion thermometer

The immersion temperature sensor used in this study is a Rosemount Model 102CH2AF total temperature probe (de-iced model). The instrument directly measures the total temperature through thermal relaxation of a platinum resistance wire contained within a housing designed to minimize wetting errors by inertially separating water particles from the air prior to measurement. The total temperature is a sum of the ambient air temperature, the dynamic heating due to the deceleration of air within the instrument housing, evaporational cooling if the sensor is wet, and any internal heating errors (e.g., conduction, self-heating, radiative transfer, and deicing heat). Lawson (1988) discussed the latter and argued that their contribution is negligible in well-designed temperature sensors.

The Rosemount sensor has been shown to perform well in clear air, but to typically suffer from wetting errors in clouds and precipitation (Lenschow and Pennell 1974; LeMone 1980; Jorgensen and LeMone 1989; Lawson and Cooper 1990). In clear air, the desired ambient air temperature is easily attained by removing the dynamic heating component via

$$T_m = T_a + r_e \frac{U^2}{2c_p}, \tag{1}$$

where T_m is the measured temperature at the surface of the sensing element, T_a is the ambient air temperature, U is the aircraft true airspeed,[1] c_p is the specific heat of air at constant pressure, and r_e is the effective recovery factor of the instrument. In clouds and precipitation, a sensor that is wetted will behave more as a wet-bulb thermometer since the dynamic heating maintains a constant supply of subsaturated air to the sensor surface. Analytic corrections for a wet sensor are difficult without knowledge of the fractional surface area of the sensor that is wetted. Lawson and Cooper (1990) assumed that a completely wetted sensor will measure the wet-bulb temperature of the dynamically heated air, and thus the resulting error caused by evaporative cooling can be calculated via

$$T_{\text{wb}} - T_m = \frac{1}{AP_s}\left[\frac{P_s}{P_o}e_o - e_s(T_{\text{wb}})\right], \tag{2}$$

where T_{wb} is the wet-bulb temperature at the sensor surface, $T_{\text{wb}} - T_m$ is the measured temperature error due to instrument wetting, P_o and e_o are the total pressure and vapor pressure in the ambient air stream, P_s and $e_s(T_{\text{wb}})$ are the total pressure and saturation vapor pressure at the sensor surface, and A is the psychometric parameter for a cylindrical sensor given by

$$A = \frac{c_p}{\epsilon L_v}\left(\frac{S_c}{P_r}\right)^{0.56}\left[1 - \frac{\epsilon e_s(T_{\text{wb}})}{P_o}\right] \tag{3}$$

where ϵ is the ratio of molecular weights of water to air, L_v is the latent heat of vaporization, S_c is the Schmidt number, and P_r is the Prandtl number. Therefore, the instrument wetting error magnitude of a well-designed immersion sensor ($r_e \sim 1.0$) will be a function of the fractional area of the sensor surface that is wetted, the true air speed, and the ambient temperature, pressure, and relative humidity.

Figure 1 shows theoretical temperature errors for a completely wetted sensor assuming a recovery factor[2]

[1] The true airspeed is a function of Mach number and the ambient air temperature.

[2] The effective recovery factor of the Rosemount 102 instrument is ~0.975 under typical flight conditions, and an assumption of 1.0 would only introduce an error of ~0.1 K to Eq. (2). For a further discussion of r_e see Lawson and Cooper (1990).

Unauthenticated | Downloaded 02/22/24 05:18 AM UTC

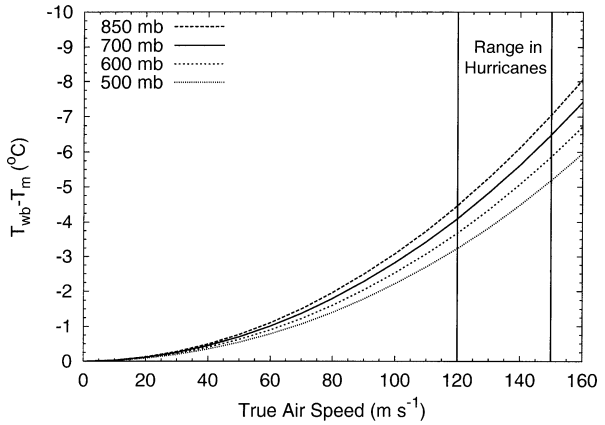

FIG. 1. Theoretical immersion sensor temperature errors ($T_{wb} - T_m$) calculated from Eq. (2) for a completely wetted sensor at 850 mb (long dashed), 700 mb (solid), 600 mb (short dashed), and 500 mb (dotted). Values were determined assuming an effective recovery factor of 1.0 and a saturated mean tropical atmosphere from Jordan (1958b). The vertical lines represent the range of true air speeds during hurricane penetrations.

of 1.0 and a saturated mean tropical atmosphere (Jordan 1958b). Errors from sensor wetting can be as large as 7°C at typical true airspeeds. Furthermore, errors will be ~0.5°C larger if the ambient air is 10% subsaturated. A completely ice-covered sensor will experience errors up to 1.0°C larger depending upon ambient relative humidity. Additional errors on the order of 1°–2°C can result if the inner housing surface becomes wetted or ice covered (R. A. Black 1999, personal communication). Therefore, we estimate that at hurricane penetration true airspeeds, the maximum temperature errors due to wetting may be as large 7°C below the freezing level and up to 10°C above the freezing level. Errors for a partially wetted sensor will, of course, be smaller.

De-iced Rosemount sensors can suffer from an additional source of error above the freezing level if the internal airflow is reduced. The de-icing heater directly heats only the leading edges of the housing but maintains ice-free conditions on all surfaces within the housing via thermal conduction. During normal operation, airflow through the housing suppresses the heated boundary layer (that results from the thermal conduction) and minimizes any heating errors down to negligible magnitudes. However, if a buildup of ice within the housing reduces the internal airflow, the heated boundary layer can expand and produce warm temperature errors. Such error magnitudes will likely increase with altitude and have been observed to be as large as 20°C at 150 mb (Rogers et al. 2002).

c. Immersion hygrometer

The immersion dewpoint sensor used in this study is a General Eastern Model 1011B hygrometer. The instrument directly measures the dewpoint temperature by stabilizing the temperature of a chilled mirror at the point when condensation first begins to form. Adverse wetting of the mirror is minimized by inertially separating water particles from the air prior to measurement.

Cooled-mirror hygrometers also suffer from wetting errors in clouds and precipitation. During such periods, the hygrometer will heat the mirror in an attempt to evaporate the excess water or ice, resulting in an erroneously warm dewpoint temperature (LeMone 1980). Errors equivalent to more than 2°C above saturation have been observed (Zipser et al. 1981; Jorgensen and LeMone 1989). Analytical corrections are unknown, but errors can be reduced by assuming saturated conditions if supersaturations are observed. However, if subsaturated conditions exist and supersaturations are observed, the correction could introduce a significant dewpoint error, depending upon the magnitude of the actual dewpoint depression.

d. Use of the term instrument wetting error

Throughout the remainder of this paper measurements (and subsequently calculated quantities) from the radiometer and immersion sensors are compared and their differences are referred to as instrument wetting errors, or simply errors. As shown in Table 2, each instrument has an absolute accuracy envelope within which random errors due to instrument design and operation can occur. Therefore, the absolute difference between two measurements at a given time may contain some inherent random errors and *not* be entirely due to wetting effects. Great care was taken during data processing (see section 3b) to effectively reduce random errors, and then to concentrate the analysis upon regions with either statistically significant temperature differences, or those that contained cloud water. As we shall see, the results overwhelmingly suggest that the large observed differences indeed occurred in regions where instrument wetting was possible, and are thus referred to as instrument wetting errors.

3. Data and methodology

a. Data

The flight-level data used in this study consists of 666 radial legs collected by the two NOAA WP-3D research aircraft at reference pressure levels of 850, 700, 600, and 500 mb during 79 flights into 26 Atlantic and 5 eastern Pacific hurricanes from 1984 to 1999 (see Table 3). During each flight the kinematic and thermodynamic data were recorded at a 1-Hz rate. The 1-Hz thermodynamic data, as well as corresponding radial legs processed from the 1-Hz data, were obtained from NOAA Hurricane Research Division (HRD) archive. The radial legs were previously produced at HRD using methods described in Willoughby et al. (1982), Willoughby and Chelmow (1982), and Samsury and Zipser (1995). Each radial leg extends up to 150 km from the storm center

Unauthenticated | Downloaded 02/22/24 05:18 AM UTC

TABLE 3. Inventory of Atlantic and East Pacific hurricanes, the distribution of radial legs by flight level, the number of radial legs with cloud water content (q_c) data available, the number of radial legs with at least one instrument wetting event, and the total number of instrument wetting events (IWE) for each hurricane.

			Radial legs							
Hurricane	Year	Flights	850 mb	700 mb	600 mb	500 mb	Total	with q_c	with IWE	Total IWE
Diana	1984	4	41	—	—	—	41	41	26	30
Norbert	1984	6	5	34	—	18	57	57	30	33
Danny	1985	2	8	—	—	—	8	6	3	3
Elena	1985	5	53	—	—	—	53	16	17	23
Gloria	1985	7	6	30	—	6	42	33	20	29
Juan	1985	2	14	—	—	—	14	14	5	5
Emily	1987	2	—	14	1	35	50	24	33	46
Floyd	1987	1	11	—	—	—	11	11	2	2
Gilbert	1988	5	16	28	—	—	44	44	29	37
Joan	1988	1	6	—	—	—	6	6	2	2
Dean	1989	1	—	—	8	—	8	—	4	4
Gabrielle	1989	1	—	4	—	—	4	2	—	—
Hugo	1989	4	—	—	22	4	26	16	15	15
Gustav	1990	4	6	30	—	—	36	27	8	11
Jimena	1991	3	2	17	4	—	23	20	12	12
Tina	1992	2	18	—	—	—	18	18	12	14
Emily	1993	2	—	—	—	11	11	11	6	7
Olivia	1994	2	—	—	16	—	16	16	9	14
Erin	1995	1	—	15	—	—	15	15	5	5
Iris	1995	1	—	—	7	—	7	7	5	9
Luis	1995	2	—	—	4	12	16	16	9	15
Opal	1995	1	—	—	4	—	4	4	2	3
Edouard	1996	2	—	22	—	—	22	22	21	30
Fran	1996	1	4	—	—	—	4	4	3	6
Hortense	1996	1	8	—	—	—	8	8	5	5
Lili	1996	3	5	—	—	—	5	5	2	2
Guillermo	1997	2	—	—	—	24	24	24	21	30
Bonnie	1998	3	—	—	29	—	29	—	8	8
Danielle	1998	2	—	—	26	—	26	—	2	2
Georges	1998	4	22	—	12	—	34	22	11	13
Floyd	1999	2	—	—	4	—	4	—	3	4
Total		79	225	194	137	110	666	487	331	420

and consists of storm-relative observations of the three-dimensional wind field in cylindrical coordinates, temperature, dewpoint, cloud water content (when available), geopotential height, and the aircraft location given in latitude, longitude, and time. Data within each radial leg is partitioned into 0.5-km-average bins by applying a triangular-shaped Bartlett filter (Jenkins and Watts 1968) with a 2-km window to the 1-Hz data. The temperature and dewpoint data included in the radial legs were obtained by the Rosemount and General Eastern sensors and adjusted at HRD using the ZML correction method. Furthermore, the temperatures and dewpoints were extrapolated along moist adiabats from flight level to the reference pressure level.

During inner-core penetrations, the pilots typically flew figure-four patterns with headings at approximately right angles to the wind direction. As a result, the radial legs within a given storm are evenly distributed about the storm center and convection is frequently sampled. By combining numerous radial legs from multiple storms, we believe the dataset is representative of the hurricane inner core in the lower and middle troposphere.

Cloud water content (q_c) was measured by a Johnson–Williams ''hot-wire'' probe. The sensor is a heated platinum resistance wire designed to be sensitive to drops <0.06 mm in diameter. However, numerous studies (e.g., Spyers-Duran 1968; Feind et al. 2000) have found the probe to undersample drops >0.03 mm in diameter, and thus underestimate q_c by a factor as large as 3, depending upon drop concentrations at the large end of the cloud droplet spectrum. Merceret and Schricker (1975) found that the probe did not respond well to $q_c < 0.05$ g m^{-3}. Baumgardner (1983) noted the probe can also suffer from out-of-cloud baseline drifting, and only upon drift removal is the absolute accuracy ($\pm 20\%$) attainable. Due to these limitations, and occasional sensor wire breakage, only $\sim$75% of the radial legs are accompanied by q_c data. Data from the forward scattering spectrometer probe (FSSP) and the particle measuring system (PMS) 2D-C and 2D-P probes were not available.

b. Data processing

In order to identify significant instrument wetting errors and examine their impact upon thermodynamic

Unauthenticated | Downloaded 02/22/24 05:18 AM UTC

quantities, separate radial profiles of temperature needed to be constructed from the radiometer (T_{sr}) and Rosemount (T_{rose}) data. Likewise, separate corresponding profiles of dewpoint (T_d) needed to be constructed to remove supersaturations with respect to each temperature. The resulting T_{sr} with its T_d (collectively referred to as the SR data) and the T_{rose} with its T_d (collectively referred to as the ROSE data) were then used to determine error statistics by assuming that the SR data are accurate.

Initially, a running Bartlett filter with an 11-s window was applied to the 1-Hz thermodynamic data in accordance with methods used to create the radial legs processed at HRD, and the filtered data was retained every 5 s. The filter acts to effectively reduce random errors within the data. The resulting data time series were then visually inspected to remove sections with spurious or incomplete thermodynamic data.

The time-dependent offset in the T_{sr} data was next removed from each inner-core penetration (an inbound/outbound radial leg couplet). A typical T_{sr} offset is depicted in Fig. 2a by the preprocessed profiles of T_{rose} and T_{sr} for a penetration through Hurricane Gilbert at 700 mb from 0959–1029 UTC 14 September 1988. The offset ($\sim$1.0°C) is most notable in the subsaturated regions (30–50 km) where instrument wetting did not occur. Previous studies (Jorgensen and LeMone 1989; Lucas et al. 1994; Wei et al. 1998) have used the clear air sections of each penetration to calculate and remove an average offset from the T_{sr} data. Such a method is difficult to apply to hurricane inner-core data since the aircraft can remain in clouds and precipitation for several hours (during which the T_{sr} offset can change). Visual inspection of the data indicated that T_d either equaled or exceeded T_{rose} (indicative of instrument wetting) in most regions containing q_c but not in the majority of regions containing only precipitation (as indicated by radar). Consequently, the offset was determined from data along each penetration during which $T_{rose} - T_d > 0.2$°C and the aircraft roll was less than $\pm 3.0°$. The 0.2°C dewpoint depression threshold acts as a time lag to permit sensors to completely dry after wetting (Wei et al. 1998). The roll threshold minimizes possible T_{sr} errors (as discussed in section 2a). The offset is calculated through linear regression of the T_{sr} and T_{rose} data that satisfied these criteria (see Fig. 2b). If the linear correlation coefficient (r) was larger than 0.96, the regression equation was used to remove the offset from the T_{sr} data of that penetration. If r was less than 0.96, the profiles of T_{sr} were not constructed and the penetration was discarded. The strict criteria for r was used to effectively minimize differences between T_{sr} and T_{rose} in subsaturated air.

Next, separate T_d profiles were determined for each of the T_{rose} and T_{sr} profiles. Measured dewpoints were adjusted to saturation when T_d exceeded either T_{rose} or T_{sr}, respectively. Otherwise dewpoints were maintained as observed. Then, the SR and ROSE data were extrapolated along a moist adiabat to the reference pressure level in accordance with methods used to create the radial leg dataset.

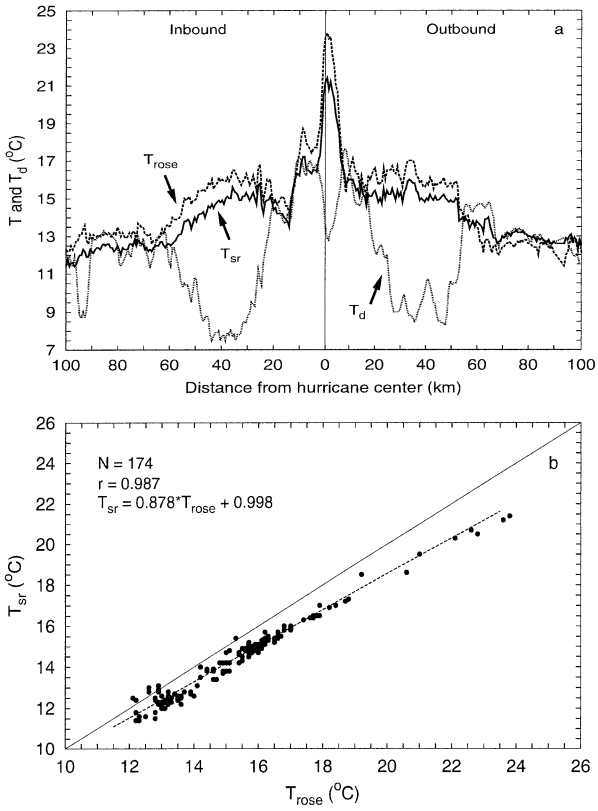

FIG. 2. (a) Storm-relative profiles of preprocessed radiometric temperature T_{sr} (solid), Rosemount temperature T_{rose} (dashed), and dewpoint T_d (dotted) for one penetration through Hurricane Gilbert at 700 mb from 0959–1029 UTC 14 Sep 1988; (b) correlation of T_{sr} with T_{rose} using only data that satisfied the dewpoint and roll criteria. The dashed line in (b) represents the best fit linear regression equation, and the variables r and N are the correlation coefficient and the number of data points, respectively. See text for descriptions of dewpoint and roll criteria. Note in (a) the $\sim$1°C offset between the preprocessed T_{sr} and T_{rose} in the subsaturated regions.

Finally, the resulting SR and ROSE profiles were fit to the 0.5-km storm-relative grid of the radial legs. Linear interpolation was used when data times did not match (temporal deviations were 1–2 s). Spurious T_{sr} spikes were removed through consideration of q_c and aircraft roll magnitude. The T_{sr} data were deemed representative of flight level if 1) the aircraft roll was less than $\pm 3.0°$, and either no q_c data was available, or q_c was less than 0.10 g m^{-3}; 2) the aircraft roll was less than $\pm 10.0°$ and q_c ranged from 0.10 to 0.20 g m^{-3}; 3) q_c was greater than or equal to 0.20 g m^{-3} regardless of aircraft roll. These criteria were determined after considerable trial and error, but are in agreement with Albrecht et al. (1979) regarding the variation in pathlength of the observed radiation with respect to q_c. If the T_{sr} data were not considered representative of flight level,

Unauthenticated | Downloaded 02/22/24 05:18 AM UTC

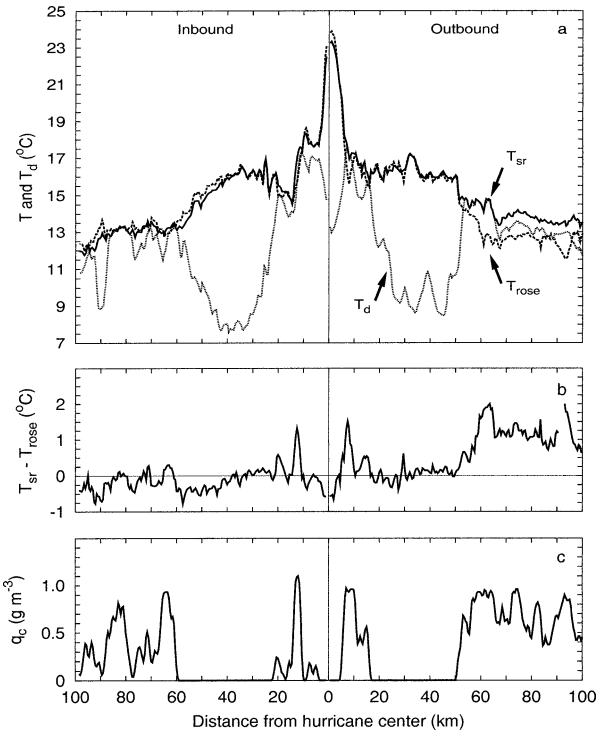

FIG. 3. Storm-relative profiles of processed (a) radiometric temperature T_{sr} (solid), Rosemount temperature T_{rose} (dashed), dewpoint T_d (dotted), (b) $T_{sr} - T_{rose}$, and (c) cloud water content q_c for the same penetration through Hurricane Gilbert shown in Fig. 2. Note that T_{sr} and T_{rose} are in good agreement outside cloud, but differ by up to 2°C in cloud.

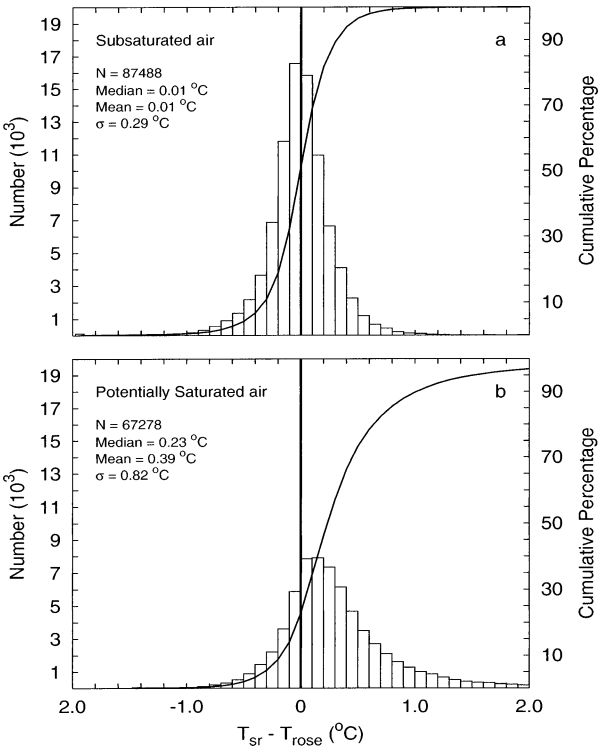

FIG. 4. Histogram of $T_{sr} - T_{rose}$ in (a) subsaturated and (b) potentially saturated air for the entire dataset after processing. Subsaturated air is defined by a dewpoint depression with respect to T_{rose} greater than 0.2°C, while potentially saturated air does not satisfy the subsaturation criteria. The solid lines represent the cumulative percentages of each distribution.

a linear average was taken between the nearest two acceptable data points (typically within 1 km).

Shown in Fig. 3 are the resulting T_{rose}, T_{sr}, T_d (from the SR data), the difference between T_{sr} and T_{rose}, and q_c for the same penetration through Hurricane Gilbert shown in Fig. 2. The T_{sr} and T_{rose} are now in good agreement in subsaturated regions (outside cloud). However, evidence of instrument wetting errors ($T_{sr} - T_{rose} > 1.0$ and $T_d > T_{rose}$) can be found in both eyewall clouds (at 10 km) and the rainband on the outbound leg (at distances >60 km). It should be noted that the presence of q_c does not directly indicate that significant instrument wetting errors are occurring. For example, the $T_{sr} - T_{rose}$ difference remains less than ±0.5°C during the majority of the rainband passage on the inbound leg.

Shown in Fig. 4 are the distributions of $T_{sr} - T_{rose}$ in subsaturated and ''potentially saturated'' air for the entire processed dataset. Data that do not satisfy the dewpoint depression criteria used above are referred to as potentially saturated because the T_d either equals or exceeds the T_{rose}, but may not equal or exceed T_{sr}. The temperature differences in subsaturated air (Fig. 4a) were normally distributed with a mean difference of 0.01° and a standard deviation (σ) of 0.29°C. Over 90% of T_{sr} are within 0.5°C of T_{rose}. This agreement suggests that the absolute accuracy of the radiometer can be achieved during aircraft operation once the time-dependent offset is removed from the data. In contrast, the temperature difference distribution in potentially saturated air (Fig. 4b) was positively skewed with a mean difference of ~0.4°C. This implies that while T_{sr} and T_{rose} are occasionally in good agreement through convection, significant instrument wetting errors exist in T_{rose} data.

Clearly, this processing method has shortcomings. First, if the dewpoint remains less than the temperature during instrument wetting an erroneously high dewpoint will never be detected. Second, assuming saturation when observed dewpoints exceed temperatures may erroneously overestimate dewpoints in subsaturated air (where precipitation may have induced the wetting). Third, the T_{sr} bias was removed using data, not in clear air, but from level and subsaturated regions that may have contained liquid water, and thus instrument wetting errors. Eastin (1999) examined this using a subset of radial legs with q_c available. The T_{sr} offsets were separately determined and removed using the dewpoint depression criteria and the absence of q_c. The resulting mean difference in T_{sr} was 0.02°C with a standard deviation of only 0.1°C. Therefore, the T_{sr} offset removal using the dewpoint depression criteria is believed to be

Unauthenticated | Downloaded 02/22/24 05:18 AM UTC

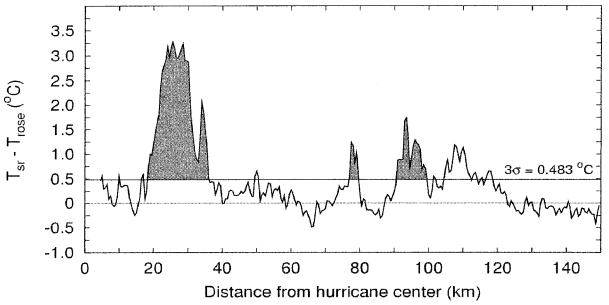

FIG. 5. Illustration of the instrument wetting event definition from a radial leg in Hurricane Guillermo at 500 mb from 2333–2350 UTC 3 Aug 1997. An instrument wetting event is defined as a region with the Rosemount temperature T_{rose} continuously cooler than radiometric temperature T_{sr} by at least three standard deviations (3σ) of that penetration's $T_{sr} - T_{rose}$ in subsaturated air (dewpoint depression with respect to T_{rose} greater than 0.2°C) for at least 2.5 km, and the event is separated from another by 10 km. The shaded regions indicate identified IWE. Note that the $T_{sr} - T_{rose}$ near 110 km exceeded 3σ for ~10 km, but was less than 10 km from the event near 95 km with a larger $T_{sr} - T_{rose}$ maximum. As a result, only the larger event was identified.

as effective as using data in clear air. Furthermore, the dewpoint depression criteria can accurately remove the T_{sr} offset when the aircraft remains in clouds and precipitation for an extended period of time, or when no radar or microphysical data is available. Finally, the radiometer measurements may be erroneously low in subsaturated regions (see section 2b) regardless of whether or not the Rosemount sensor is wetted. Such errors in T_{sr} are reduced by using data in subsaturated regions to initially remove any radiometer bias. Furthermore, Fig. 4 suggests that regions in which T_{sr} is significantly lower than T_{rose} are rare.

c. Definition of an instrument wetting event

Each of the 666 radial legs were examined to identify regions of *significant* instrument wetting error in the T_{rose} data. To eliminate subjectivity, the following specific criteria were adopted. Instrument wetting events (IWE) were defined as regions where T_{rose} was continuously cooler than T_{sr} by at least three standard deviations of that penetration's $T_{sr} - T_{rose}$ value in subsaturated air ($3\sigma \approx 0.5$°C) for at least 2.5 km, and each instrument wetting event was required to be separated from another by 10 km (see Fig. 5). When two potential IWE are within 10 km of each other, the event with the largest maximum $T_{sr} - T_{rose}$ is selected. These strict criteria ensured that temperature differences were indeed instrument wetting errors, and that each event was distinct. The use of smaller critical diameters increased the number of IWE, but did not have a significant effect (according to a Student's *t*-test) upon average thermodynamic error magnitudes. The use of lower critical temperature differences increased the number of IWE while decreasing the average error magnitudes, but could not ensure that all the apparent IWE were significant instrument wetting.

A total of 420 IWE were identified in the 666 radial legs (Table 3). The number of IWE per radial leg ranged from 0 to 3, but at least 1 event was present in 331 radial legs, or roughly half of all radial legs. Some hurricanes (Diana 1984, Norbert 1984, Emily 1987, Gilbert 1988, Hugo 1989, Tina 1992, Emily 1993, Olivia 1994, Iris 1995, Luis 1995, Edouard 1996, Fran 1996, Hortense 1996, Guillermo 1997, and Floyd 1999) contained IWE in more than 50% of their radial legs, whereas Hurricane Gabrielle (1989) was completely without IWE. Nearly two-thirds of the IWE occur in intense hurricanes (Category 3, 4, and 5 on the Saffir–Simpson scale), and the events are evenly distributed among the quadrants with respect to motion.

Several characteristics of IWE were determined. These included the average and maximum errors in temperature (T), specific humidity (q), virtual potential temperature (θ_v), and equivalent potential temperature (θ_e), diameter (or radial distance along the flight track), average vertical velocity (w), and average q_c. The average errors were determined by first calculating the desired quantity from each of the SR and ROSE data separately, and then taking their average difference across the event. Maximum errors were determined in a similar manner, but as the maximum 0.5-km difference within the event. Equivalent potential temperatures were calculated using the empirical formulation given by Bolton (1980).

d. Definition of vertical velocity cores

In order to determine the magnitude of thermodynamic errors within updrafts and downdrafts, the vertical velocity data was used to identify events called *cores.* Updraft and downdraft cores are defined when $|w|$ exceeds 1.0 m s^{-1} for at least 0.5 km of horizontal distance along the radial leg. These definitions are identical to those used by Samsury and Zipser (1995) and are analogous to the definitions used by Jorgensen et al. (1985). Cores were further required to contain cloud water (i.e., $q_c > 0.0$ g m^{-3}). While this criteria may remove a few cores that still contain precipitation, and thus potentially significant instrument wetting errors, the criteria more importantly removes the cores in clear air without wetting errors.

Jorgensen et al. (1985) noted that the zero vertical velocity was typically offset 0.1–0.4 m s^{-1} in nonconvective regions due to a known drift in the vertical accelerometer, and such offsets could lead to the spurious identification of updrafts and downdrafts. Therefore, prior to core identification, the leg average vertical velocity was determined from the $|w| < 1.5$ m s^{-1} data and removed. The critical value of 1.5 m s^{-1} was chosen to isolate nonconvective regions with consideration for the absolute accuracy of the computed vertical velocity (±1.0 m s^{-1}; Merceret 1982). The computed offsets were typically less than 0.3 m s^{-1}.

Unauthenticated | Downloaded 02/22/24 05:18 AM UTC

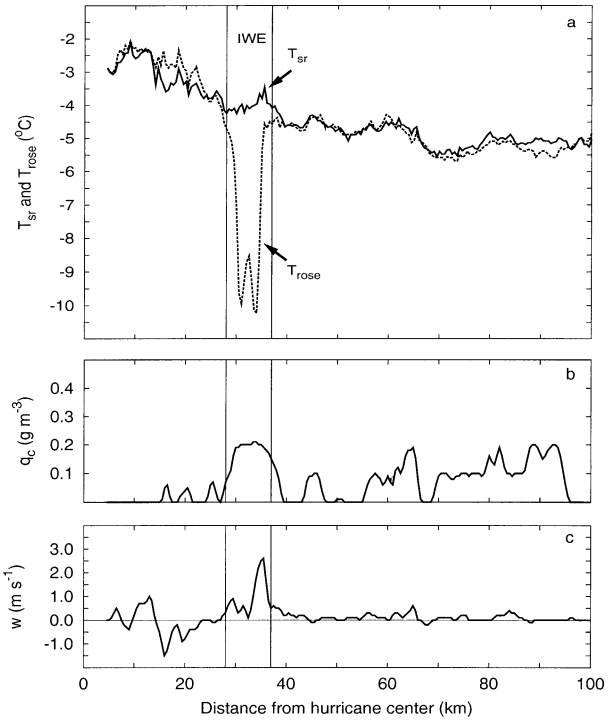

FIG. 6. Storm-relative profiles of (a) radiometric temperature T_{sr} (solid), Rosemount temperature T_{rose} (dashed), (b) cloud water content q_c, and (c) vertical velocity w for one radial leg through Hurricane Gloria at 500 mb from 2012–2044 UTC 22 Aug 1985. The vertical lines bracket the instrument wetting event identified in the eyewall.

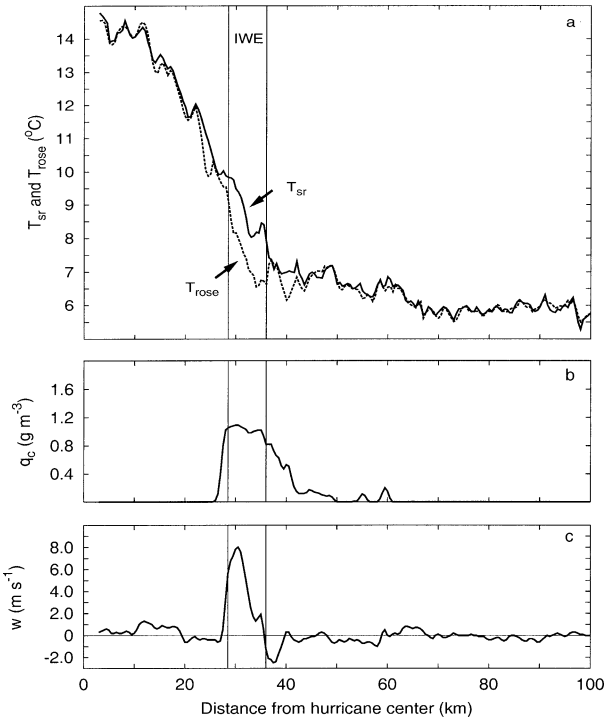

FIG. 7. Similar to Fig. 6 but for Hurricane Hugo at 600 mb from 0131–0145 UTC 22 Sep 1989.

A total of 1673 updraft cores and 948 downdraft cores that contained q_c were identified. Again, several characteristics of each core were determined. These included the average and maximum errors in T, q, θ_v, and θ_e, diameter, average and maximum w, and average q_c. The errors were determined in an analogous manner as the errors in IWE. Distributions of core diameter and average and maximum w were approximately lognormal and consistent with Jorgensen et al. (1985), suggesting that convection was well sampled.

e. Determination of eyewall and rainband regions

Each radial leg was divided into two parts in order to separately determine thermodynamic error characteristics within eyewall and rainband convection. Following procedures used by Jorgensen et al. (1985), a radial cutoff distance was subjectively determined using radar imagery and radial profiles of horizontal wind, w, and q_c to include all eyewall convection inward of this cutoff. The rainband region is outside the cutoff distance. In general the cutoff distance was ~15 km outside the radius of maximum wind (RMW). The eyewall was typically identified as the quasi-annular ring of innermost convection. If the innermost convection consisted of numerous convective bands close to one another (within 15 km), all the bands were included in the eyewall region. Concentric outer eyewalls described by Willoughby et al. (1982) were included in the rainband region if they were >20 km from a distinct inner eyewall. In minimal hurricanes, the innermost convection was typically an asymmetric band near the RMW that slightly spiraled outward. In such cases, this innermost band was included in the eyewall region. These procedures account for the variability of the eyewall radius as well as asymmetries from storm to storm.

4. Results

a. Variability of IWE

Considerable variability was found in the magnitude, shape, and diameter of IWE. Figures 6 and 7 provide two examples. The instrument wetting event at 500 mb in the eyewall of Hurricane Gloria (Fig. 6) is very pronounced with a maximum temperature error of 6.3°C and a diameter of 9.0 km that is comparable to the radial extent of the eyewall cloud. In contrast, the instrument wetting event at 600 mb in the eyewall of Hurricane Hugo (Fig. 7) is not as pronounced. The maximum temperature error is 1.7°C with a diameter of 7.5 km that is roughly half the radial extent of the eyewall cloud. Hugo's event is representative of the majority of IWE, and illustrates the difficulty in visually identifying errors from T_{rose} data alone. Both radial legs contain regions of apparent instrument wetting outside the identified IWE. Although these regions do not satisfy the strict

Unauthenticated | Downloaded 02/22/24 05:18 AM UTC

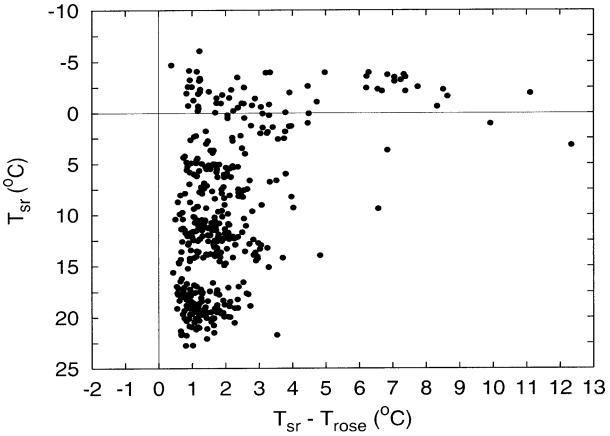

FIG. 8. Scatterplot of the maximum temperature errors ($T_{sr} - T_{rose}$) within IWE.

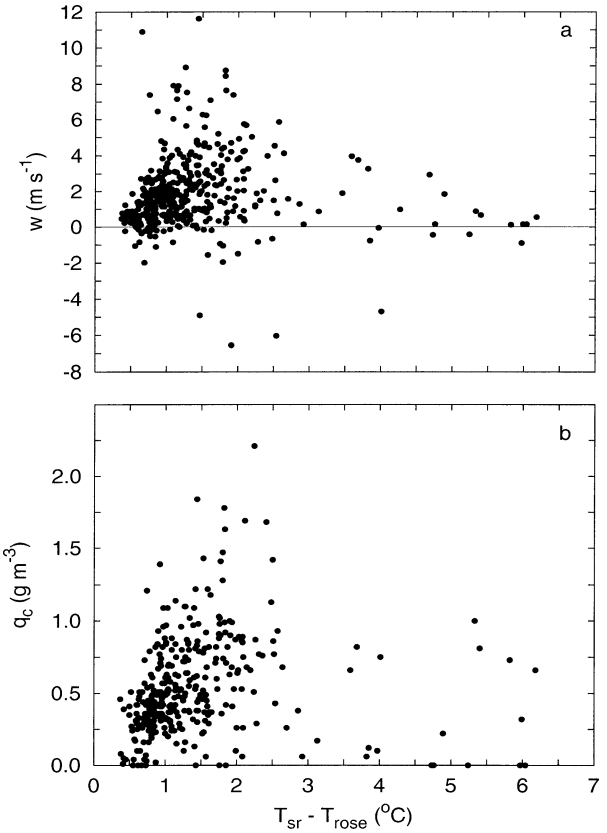

FIG. 9. Scatterplot of the average (a) cloud water content q_c and (b) vertical velocity w within IWE.

criteria for IWE, they illustrate that small (in magnitude and diameter) instrument wetting errors may frequently occur during penetrations through clouds and precipitation.

Maximum temperature errors within IWE (Fig. 8) range from 0.5°C to over 10°C. Below the freezing level, over 95% of the maximum errors are less than 3.0°C. Near the freezing level, maximum errors frequently exceed 3.0°C. This increase near the freezing level was expected due to the additional cooling that results from the melting process prior to evaporation. Note that the majority of errors exceed the Zipser et al. (1981) estimated maximum error of 1.5°C. However, maximum temperature errors rarely achieve the theoretical magnitudes (5°–10°C) predicted by Eq. (2), indicating that the Rosemount sensor is rarely wetted completely.

The largest error observed in the entire dataset was 12.3°C at 500 mb (near the freezing level) in the eyewall of Hurricane Emily (1987). A similar error magnitude was observed near the freezing level by Jorgensen and LeMone (1989) during a penetration of oceanic tropical convection (see their Fig. 7). Such extreme errors near the freezing level suggest that Rosemount sensors are highly unreliable in regions of mixed-phase hydrometeors.

Shown in Figs. 9a,b are scatterplots of average w and q_c within IWE with respect to the average temperature error. The vast majority (~90%) of IWE are dominated by updrafts, and ~95% contain cloud liquid water (see also Table 4). In addition, the average temperature error is weakly correlated with average w ($r \sim 0.2$) and average q_c ($r \sim 0.4$). Lenschow and Pennell (1974) first speculated that small cloud drops may not contain enough inertia to be effectively separated from the measured air in Rosemount sensors. Therefore, the magnitude of instrument wetting errors may be related to either the concentration of small cloud drops, or cloud water content. In studies of nonprecipitating clouds, Albrecht et al. (1979) and Lawson and Cooper (1990) found that Rosemount instrument wetting errors were weakly correlated with cloud water content. While our results are consistent with these studies, hurricane convection contains copious amounts of precipitation that could also contribute to instrument wetting errors. Note that ~5% of IWE contain no cloud water, indicating that those errors were caused entirely by precipitation-sized particles. Unfortunately, complete drop-size distributions were not available to further investigate relationships between cloud microphysics and Rosemount temperature error magnitudes.

TABLE 4. Summary of IWE by flight level with regard to location and diameter, vertical velocity (w), and cloud water content (q_c) characteristics.

	850 mb	700 mb	600 mb	500 mb
Total IWE	114	134	82	90
IWE in eyewall region	93	98	63	71
IWE in rainband region	16	33	17	17
IWE in updrafts	99	123	74	73
IWE in downdrafts	15	11	8	17
IWE with q_c	91	106	55	78
IWE without q_c	4	4	3	5
IWE with no q_c data	19	24	24	7
Mean w (m s^{-1})	0.9	2.0	2.2	2.4
Mean q_c (g m^{-3})	0.39	0.52	0.68	0.63
Mean diameter (km)	6.6	7.3	6.8	13.7

Unauthenticated | Downloaded 02/22/24 05:18 AM UTC

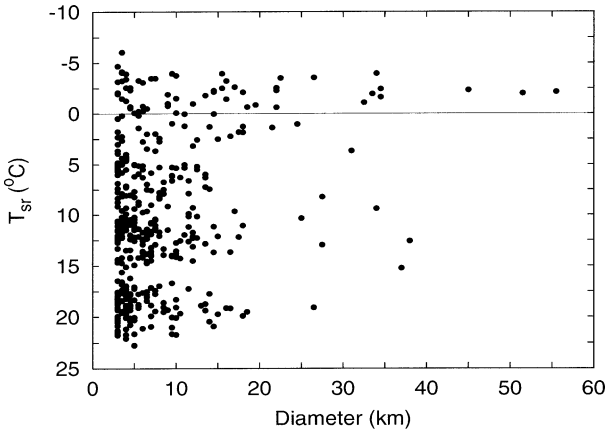

FIG. 10. Scatterplot of instrument wetting event diameters.

The majority of instrument wetting event diameters (Fig. 10) are less than 10 km with a few extending up to 55 km. The wider IWE were associated with rainband convection and may have been enhanced by stratiform precipitation. Mean diameters are ~7 km below the freezing level (see Table 4), doubling to ~14 km near the freezing level. This increase may have resulted from a buildup of ice on the sensor. Nevertheless, the majority of IWE are spatially confined to the convective scale.[3] A comparison between diameter and average temperature error (not shown) indicates a tendency ($r \sim 0.5$) for wider IWE to be associated with larger temperature errors.

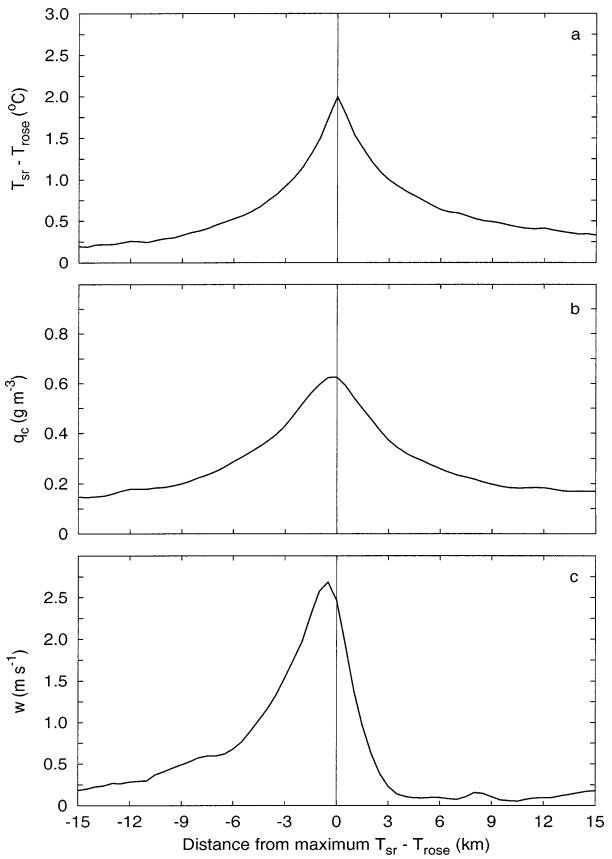

FIG. 11. Composite (a) temperature error $T_{sr} - T_{rose}$ (b) cloud water content q_c, and (c) vertical velocity w across IWE. The composites were constructed with respect to the maximum temperature error within each event. A positive (negative) distance is radially outward (inward) from the maximum error.

b. Composite radial structure of IWE

The along-track (i.e., radial) structure of a ''typical'' instrument wetting event is illustrated by compositing all IWE with respect to their maximum temperature error. Composites were initially constructed at each pressure level, but because these showed little variability in structure, all IWE were combined. Differences in error magnitudes with height were evident and are discussed in section 4c. Shown in Fig. 11 are composites of $T_{sr} - T_{rose}$, w, and q_c for a typical instrument wetting event. Temperature errors (Fig. 11a) are nearly symmetric about the ~2.0°C maximum. Errors decrease to ~0.5°C within 6 km while remaining statistically significant at the 99% confidence level.

The composite profile of q_c across a typical instrument wetting event (Fig. 11b) is also symmetric about a collocated maxima. The positive correlation between q_c and $T_{sr} - T_{rose}$ provides further evidence that instrument wetting errors increase with cloud water content, but also suggests that (on average) no temporal or spatial lag exists between the aircraft encountering the maximum q_c and the occurrence of the maximum temperature error. Separate composites of IWE encountered on inbound and outbound radial legs were constructed and confirmed the absence of a lag.

The composite profile of w (Fig. 11c) is asymmetric with a maximum ~0.5–1.0 km radially inside the temperature error maximum. The sharp decrease in w outside the updraft maximum is a result of sporadic convective downdrafts commonly found at radii just beyond updrafts in hurricane convection (Jorgensen et al. 1985). These downdrafts typically contain large precipitation water contents that fell out of the adjacent outward-sloping updrafts aloft. The offset distance and direction is consistent with the location of the radial maximum *total* liquid water that is typically found either on the outside edge of hurricane updrafts or in adjacent convective downdrafts (Black and Hallett 1986). This further suggests that precipitation particles may contribute to Rosemount sensor errors.

[3] The dominance of convective scale diameters may partially be an artifact of the aircraft crossing hurricane convective bands rather than traversing along the convective band. Along-band flight tracks would likely produce much larger diameters.

Unauthenticated | Downloaded 02/22/24 05:18 AM UTC

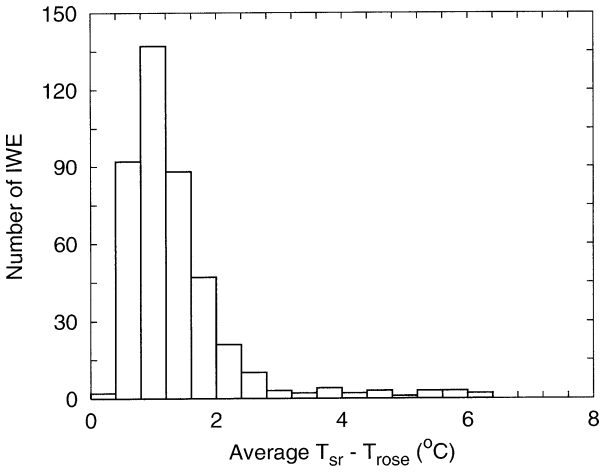

FIG. 12. Distribution of average temperature errors ($T_{sr} - T_{rose}$) within IWE.

c. Thermodynamic errors in IWE

Distributions of the average T, q, θ_v, and θ_e errors within IWE were compiled at each pressure level. Shown, for example, in Fig. 12 is the distribution of average temperature error. All thermodynamic error distributions at each pressure level were skewed toward larger values as in Fig. 12. As a result, the distributions are not shown individually, but rather the mean, median (50% level), and upper 10% (<90% of the population) values of each distribution are extracted at each pressure level and presented in Table 5.

In general, all thermodynamic errors within IWE tend to increase with height. The increases are likely a combination of an increase in average q_c with height (see Table 4) and phase change effects near the freezing level. Median average T, q, θ_v, and θ_e errors are 1–2°C, 0.8 g kg^{-1}, 1–3 K, and 3–5 K, respectively. Mean average error values are ~10%–20% larger than the median values, while the upper 10% of average error magnitudes are ~40%–50% larger than the median values. These magnitudes represent substantial errors in thermodynamic parameters used to evaluate hurricane convection and evolution.

Tables 3 and 4 indicate that the majority of IWE are located in eyewalls and intense hurricanes. Jorgensen et al. (1985) found updrafts to be stronger in eyewalls than in rainbands, and Black (1993) noted that eyewall updrafts are typically stronger in intense hurricanes. Our results indicate that thermodynamic errors are weakly correlated with vertical velocity. Therefore, are error magnitudes also larger in eyewalls and intense hurricanes? Stratifications of the IWE with respect to intensity and inner-core region were made, but no *systematic* differences in error magnitude were found, despite the discrepancies in numbers of IWE. The lack of variability suggests that the statistics in Table 5 are not unique to hurricane convection.

d. Thermodynamic errors in convective cores

Distributions of the average T, q, θ_v, and θ_e errors within updraft and downdraft cores were initially compiled at each pressure level. All thermodynamic error distributions were skewed toward larger values. As before, error distributions are not shown individually, but rather the mean, median, and upper 10% values of each distribution are extracted at each pressure level and presented in Tables 6 and 7 for updrafts and downdrafts, respectively.

Thermodynamic errors within updraft cores tend to increase with height. Median average temperature errors either equal or exceed the absolute accuracy of the radiometer (±0.5°C) indicating that the majority of updraft cores within the hurricane inner core contain significant thermodynamic errors. Mean average errors are ~20% larger than the median values, and are statistically significant at the 99% confidence level. The upper 10% of average errors are two to four times larger than the median values with T, q, θ_v, and θ_e errors exceeding 1.0°C, 1.0 g kg^{-1}, 1.3 K, and 4.5 K, respectively.

Thermodynamic errors within downdraft cores show less vertical variation and are smaller in magnitude. Median average temperature errors are within the absolute accuracy of the radiometer as only 35% of maximum T errors exceed 0.5°C. Hence, the majority of downdraft cores do not contain substantial thermodynamic errors. However, the mean average errors are positive and statistically significant at the 99% level. The upper 10% of average T, q, θ_v, and θ_e errors exceeded 0.8°C, 0.5 g kg^{-1}, 1.0 K, and 2.5 K, respectively. Therefore, a considerable fraction of downdraft cores within the hurricane inner core contain significant thermodynamic errors.

Linear correlation coefficients between core average

TABLE 5. Mean, median (50%), and upper 10% values of instrument wetting event average thermodynamic error calculated from the SR and ROSE data and stratified by flight level. Bold mean values are statistically significant at the 99% confidence level.

Level	T error (°C)			q error (g kg^{-1})			θ_v error (K)			θ_e error (K)		
(mb)	Mean	50%	90%	Mean	50%	90%	Mean	50%	90%	Mean	50%	90%
500	**2.2**	1.8	4.8	**1.0**	0.9	1.9	**2.9**	2.4	4.9	**6.1**	5.1	9.7
600	**1.3**	1.2	2.0	**0.9**	0.8	1.4	**1.7**	1.6	2.5	**4.4**	4.1	7.1
700	**1.2**	1.1	1.9	**0.9**	0.8	1.7	**1.5**	1.4	2.4	**4.4**	4.1	7.4
850	**0.9**	0.9	1.5	**0.9**	0.8	1.5	**1.1**	1.0	1.9	**3.8**	3.5	6.4

Unauthenticated | Downloaded 02/22/24 05:18 AM UTC

TABLE 6. Similar to Table 5 but for average thermodynamic errors in updraft cores.

Level (mb)	T error (°C)			q error (g kg^{-1})			θ_v error (K)			θ_e error (K)		
	Mean	50%	90%	Mean	50%	90%	Mean	50%	90%	Mean	50%	90%
500	**1.0**	0.7	2.4	**0.5**	0.3	1.2	**1.3**	0.9	3.2	**2.8**	1.8	7.0
600	**0.6**	0.6	1.3	**0.4**	0.3	1.0	**0.8**	0.8	1.7	**2.1**	1.8	4.5
700	**0.6**	0.5	1.3	**0.5**	0.4	1.0	**0.8**	0.7	1.6	**2.1**	1.7	4.8
850	**0.5**	0.4	1.0	**0.5**	0.4	1.0	**0.6**	0.5	1.3	**2.0**	1.7	4.5

temperature error and q_c are roughly 0.3 in both updrafts and downdrafts, providing further evidence that instrument wetting errors tend to increase with cloud water content. Core average temperature error is also weakly correlated with average updraft strength ($r = 0.24$), but not with average downdraft strength ($r = -0.08$). Stratifications of cores with respect to intensity and inner-core location again revealed no systematic differences in thermodynamic error magnitudes.

e. Evaluation of the ZML correction method

The ZML correction method has been used in studies of hurricane mesoscale structure and convection (see Table 1) to account for instrument wetting errors before radiometers were available. The method is based upon the premise that the immersion temperature and dewpoint sensors are simultaneously wetted in a saturated environment, resulting in errors that are equal in magnitude, but opposite in sign. The errors are detected as periods when T_d exceeds T_{rose}, and are removed by adjusting the temperature to the average of the erroneous T_{rose} and T_d, while assuming saturation. In practice, the errors may not be equal and opposite due to dissimilar sensor wetting or dissimilar instrument response to equivalent wetting. Therefore, the method was devised as a crude means to *reduce* instrument wetting errors, and was never intended to completely remove the errors (E. J. Zipser 1999, personal communication). The ZML correction method is evaluated using the independent and more accurate temperature measurement provided by the radiometer.

The ZML temperature correction method was applied to the radial leg data during initial processing at HRD. Thus, the temperature (referred to as T_{zml}) and dewpoint values (collectively referred to as the ZML data) provided in the archived radial legs are used for this analysis. The method's performance is evaluated in the previously identified IWE and convective cores.

Shown in Fig. 13 are the resulting temperature errors ($T_{\text{sr}} - T_{\text{zml}}$) after the ZML method was applied to the maximum temperature errors ($T_{\text{sr}} - T_{\text{rose}}$) within IWE. The method corrected only 34% of the errors to within the absolute accuracy of the radiometer (±0.5°C). Over 60% of the maximum errors were ''undercorrected'' and remain greater than 0.5°C after the ZML method was applied. Roughly 2% of the errors were ''overcorrected.'' The under(over)-corrections suggest that T_d errors were less(more) than T_{rose} errors. When the average $T_{\text{sr}} - T_{\text{zml}}$ errors across IWE were compiled, only 50% were reduced below ±0.5°C. The mean, median, and upper 10% thermodynamic error statistics for IWE after the ZML correction method was applied (not shown) were ~30%–50% smaller than their corresponding values before the ZML method was applied (see Table 5). However, all mean average errors within IWE remained positive and statistically significant at the 95% level. Therefore, the ZML correction method *reduced* errors as intended, but was ineffective at *removing* the majority of significant errors.

Application of the ZML method to convective cores containing cloud water effectively removed the majority (~70%) of significant errors. The statistics presented in Tables 6 and 7 (without application of the ZML correction) were reduced by ~30%–50%. However, mean maximum and average errors remained positive and statistically significant at the 95% level since ~35% of updrafts and ~25% of downdrafts still contained T errors greater than 0.5°C. Thus, a considerable fraction of significant thermodynamic errors remained in updrafts and downdrafts after the ZML method was applied.

5. Summary and concluding remarks

Immersion thermometers that have historically been used on research aircraft during hurricane penetrations can become wet in clouds and precipitation. As a result, the subsaturated conditions maintained at the sensor surface (through dynamic heating) permit evaporational cooling that induces an erroneously low temperature measurement. Radiometric thermometers, however, can provide more accurate measurements through both clear and cloudy air. Concurrent flight-level measurements made by radiometric and Rosemount immersion thermometers during 79 flights into 31 hurricanes have been used to identify events of significant instrument wetting–induced error in the Rosemount data, assuming the radiometer data are accurate. The criteria for instrument wetting events (IWE) required the temperature difference between the radiometer and Rosemount data to exceed three standard deviations of their difference in subsaturated air (3σ is typically 0.5°C) for at least 2.5 km, and each event to be separated from any other by at least 10 km. Statistics of IWE properties and thermodynamic errors are summarized at four pressure levels from 850 to 500 mb. Statistics of thermodynamic

Unauthenticated | Downloaded 02/22/24 05:18 AM UTC

TABLE 7. Similar to Table 5 but for average thermodynamic errors in downdraft cores.

Level (mb)	T error (°C)			q error (g kg^{-1})			θ_v error (K)			θ_e error (K)		
	Mean	50%	90%	Mean	50%	90%	Mean	50%	90%	Mean	50%	90%
500	**0.5**	0.2	1.6	**0.2**	0.1	0.8	**0.7**	0.3	2.1	**1.5**	0.4	4.8
600	**0.2**	0.1	0.8	**0.1**	0.1	0.5	**0.2**	0.1	1.1	**0.7**	0.3	2.5
700	**0.2**	0.1	0.9	**0.1**	0.1	0.5	**0.3**	0.2	1.1	**0.8**	0.3	2.5
850	**0.2**	0.2	0.8	**0.2**	0.1	0.7	**0.3**	0.2	1.0	**1.0**	0.5	3.2

errors within vertical velocity cores, defined in an identical manner as Samsury and Zipser (1995), are summarized as well. The correction method proposed by Zipser et al. (1981) to reduce such errors was evaluated. Our findings reveal that

1) Rosemount instrument wetting errors were frequently found within hurricane innercore convection. At least one instrument wetting event was identified in ~50% of the radial legs. The majority (~70%) of IWE were associated with eyewall convection in intense hurricanes and were confined to scales smaller than 10 km.
2) Over 90% of IWE were dominated by updrafts with cloud water, and temperature errors were weakly correlated with both vertical velocity ($r \sim 0.2$) and cloud water ($r \sim 0.4$). These results are in agreement with Albrecht et al. (1979) and Lawson and Cooper (1990). The ~5% of IWE that did not contain cloud water indicate that precipitation also plays a role in producing instrument wetting errors.
3) Rosemount temperature errors *rarely* achieved theoretical predictions of 5°–10°C, indicating that the sensor is rarely wetted completely due to instrument design. Maximum temperature errors within IWE were typically 1°–3°C below the freezing level (850–600 mb) with errors of 2°–5°C common near the freezing level (500 mb) due to the additional cooling that results from ice melting.
4) Distributions of average T, q, θ_v, and θ_e errors within IWE were found to be skewed toward larger values. Median average errors indicated that the thermodynamic quantities were typically too low by ~1.0°C, ~0.8 g kg^{-1}, ~1.5 K, and ~4.5 K, respectively. The upper 10% of average errors exceeded 1.5°C, 1.5 g kg^{-1}, 2.0 K, and 6.5 K, respectively. All error magnitude statistics increased with altitude.
5) Distributions of average thermodynamic errors within vertical velocity cores were also skewed toward larger values. The majority of updraft cores (~65%) and a considerable fraction of downdraft cores (~35%) contained T, q, θ_v, and θ_e errors in excess of 0.5°C, 0.5 g kg^{-1}, 0.6 K, and 2 K, respectively. All error magnitude statistics increased with altitude. Errors were weakly correlated ($r \sim 0.2$) with updraft strength, but no relation was found with downdraft strength.
6) Application of the correction method proposed by Zipser et al. (1981) reduced the error statistics in IWE by 30°–50%, resulting in average T, q, θ_v, and θ_e errors of 0.6°C, 0.5 g kg^{-1}, 0.9 K, and 2.7 K, respectively. Zipser et al. (1981) and Barnes et al. (1983) estimated that the method would correct θ_e to within 2.0 K of the true value. Our results support their estimate. Application of the method to data within vertical cores reduced temperature errors below 0.5°C in ~70% of the cases. Therefore, the correction method should be used with caution when applied to convective scales since a considerable fraction of IWE and cores still contained significant instrument wetting errors.
7) No significant systematic differences in error magnitudes were found when either IWE or vertical velocity cores were stratified with respect to either storm intensity or region (eyewall or rainband). The lack of variability suggests that the error statistics are not particularly unique to hurricane convection, but rather are applicable to any dataset collected in deep precipitating convection by aircraft with similar instrumentation.

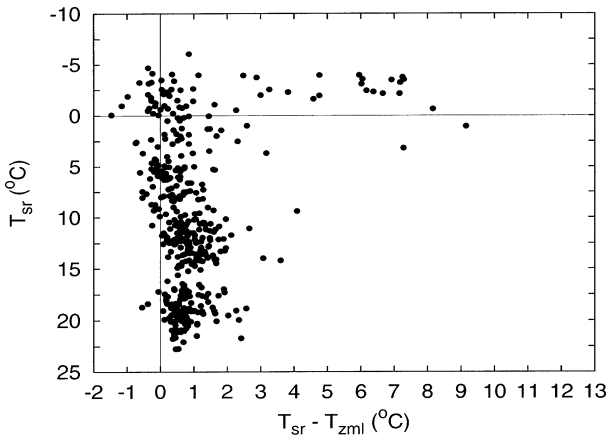

FIG. 13. Scatterplot of resulting temperature errors ($T_{sr} - T_{zml}$) after the ZML correction method was applied to the maximum temperature error within each instrument wetting event. See text for a description of the ZML correction method.

As we continue to investigate the convective structure and evolution of hurricanes (and other atmospheric sys-

Unauthenticated | Downloaded 02/22/24 05:18 AM UTC

tems) accurate in situ thermodynamic measurements will be required. To date, radiometers provide the most reliable flight-level temperature measurements in convective systems, but suffer from time-dependent offsets and complicated calibrations (Lawson and Cooper 1990). Immersion thermometers that do not suffer from instrument wetting errors have recently been developed (Lawson and Rodi 1992; Haman et al. 1997), but are not commercially available. Water vapor is measured with the least amount of accuracy. Chilled-mirror immersion hygrometers are widely used, but suffer from instrument wetting and slow response times. Infrared hygrometers (e.g., Lyman-alpha instruments) have faster response times, but suffer from drifts in calibration. With these considerations in mind, efforts toward improved aircraft thermodynamic instrumentation are needed.

A companion paper (Eastin et al. 2002) examines the implications of instrument wetting error removal upon the mean eyewall structure, buoyancy of rainband vertical motions, and vertical energy fluxes near the top of the inflow layer.

Acknowledgments. The authors are grateful to the flight crews and scientists from the NOAA Aircraft Operations Center and Hurricane Research Division for their dedicated efforts over the past two decades to collect the flight-level data used in this study. We appreciate the efforts of Hugh Willoughby and Ed Rahn in making the data available to us. We would also like to thank Bob Black and Richard McNamara for many helpful discussions through the course of this work. The editorial comments made by Jill Schaefer are appreciated. The comments of three anonymous reviews were very beneficial and improved this paper. This research was partially supported by NSF Grant ATM-9616818 and NOAA Grant NA67RJ0152.

REFERENCES

Albrecht, B. A., S. K. Cox, and W. H. Schubert, 1979: Radiometric measurements of in-cloud temperature fluctuations. *J. Appl. Meteor.*, **18,** 1066–1071.

Barnes, G. M., and G. J. Stossmeister, 1986: The structure and decay of a rainband in Hurricane Irene (1981). *Mon. Wea. Rev.*, **114,** 2590–2601.

——, and M. D. Powell, 1995: Evolution of the inflow boundary layer of Hurricane Gilbert (1988). *Mon. Wea. Rev.*, **123,** 2348–2368.

——, E. J. Zipser, D. Jorgensen, and F. Marks Jr., 1983: Mesoscale and convective structure of a hurricane rainband. *J. Atmos. Sci.*, **40,** 2127–2137.

——, J. F. Gamache, M. A. LeMone, and G. J. Stossmeister, 1991: A convective cell in a hurricane rainband. *Mon. Wea. Rev.*, **119,** 776–794.

Baumgardner, D., 1983: An analysis and comparison of five water droplet measuring devices. *J. Climate Appl. Meteor.*, **22,** 891–910.

Black, M. L., 1993: Comparisons of tropical cyclone intensity with eyewall vertical velocities. Preprints, *20th Conf. on Hurricanes and Tropical Meteorology,* San Antonio, TX, Amer. Meteor. Soc., 520–523.

Black, P. G., and G. J. Holland, 1995: The boundary layer of Tropical Cyclone Kerry (1979). *Mon. Wea. Rev.*, **123,** 2007–2028.

Black, R. A., and J. Hallett, 1986: Observations of the distribution of ice in hurricanes. *J. Atmos. Sci.*, **43,** 802–822.

——, H. B. Bluestein, and M. L. Black, 1994: Unusually strong vertical motions in a Caribbean hurricane. *Mon. Wea. Rev.*, **122,** 2722–2739.

Bolton, D., 1980: The computation of equivalent potential temperature. *Mon. Wea. Rev.*, **108,** 1046–1053.

Colon, J. A., 1964: On the structure of Hurricane Helene (1958). National Hurricane Research Project Rep. 72, U.S. Weather Bureau, 56 pp.

Eastin, M. D., 1999: Instrument wetting errors in hurricanes and a re-examination of inner-core thermodynamics. Dept. Atmospheric Science Paper 683, Colorado State University, Fort Collins, CO, 203 pp. [Available from Dept. Atmospheric Science, Colorado State University, Fort Collins, CO 80523.]

——, P. G. Black, and W. M. Gray, 2002: Flight-level instrument wetting errors in hurricanes. Part II: Implications. *Mon. Wea. Rev.*, **130,** 842–851.

Feind, R. E., A. G. Detweiler, and P. L. Smith, 2000: Cloud liquid water measurements on the Armored T-28: Intercomparisons between Johnson–Williams cloud water meter and CSIRO (King) liquid water probe. *J. Atmos. Oceanic Technol.*, **17,** 1630–1638.

Frank, W. M., 1984: A composite analysis of the core of a mature hurricane. *Mon. Wea. Rev.*, **112,** 2401–2420.

Gentry, R. C., 1964: A study of hurricane rainbands. National Hurricane Research Project Rep. 69, U.S. Weather Bureau, 85 pp.

Gray, W. M., 1965: Calculations of cumulus draft velocities in hurricanes from aircraft data. *J. Appl. Meteor.*, **4,** 463–474.

——, and D. J. Shea, 1973: The hurricane's inner core region. II. Thermal stability and dynamic characteristics. *J. Atmos. Sci.*, **30,** 1565–1576.

Haman, K. E., A. Makulski, and S. P. Malinowski, 1997: A new ultrafast thermometer for airborne measurements in clouds. *J. Atmos. Oceanic Technol.*, **14,** 217–227.

Hawkins, H. F., and D. T. Rubsam, 1968: Hurricane Hilda, 1964. II. Structure and budgets of the hurricane on October 1, 1964. *Mon. Wea. Rev.*, **96,** 617–636.

——, and S. M. Imbembo, 1976: The structure of a small, intense hurricane—Inez, 1966. *Mon. Wea. Rev.*, **104,** 418–442.

Hilleary, D. T., and F. E. Christensen, 1957: Instrumentation of National Hurricane Research Project aircraft. National Hurricane Research Project Rep. 11, U.S. Weather Bureau, 71 pp.

Jenkins, G. M., and D. G. Watts, 1968: *Spectral Analysis and Its Applications.* Holden-Day, 525 pp.

Jordan, C. L., 1958a: The thermal structure of the core of tropical cyclones. *Geophysica*, **6,** 281–297.

——, 1958b: Mean soundings for the West Indies area. *J. Meteor.*, **15,** 91–97.

Jorgensen, D. P., 1984a: Mesoscale and convective-scale characteristics of mature hurricanes. Part I: General observations by aircraft. *J. Atmos. Sci.*, **41,** 1268–1285.

——, 1984b: Mesoscale and convective-scale characteristics of mature hurricanes. Part II: Inner core structure of Hurricane Allen (1980). *J. Atmos. Sci.*, **41,** 1287–1311.

——, and M. A. LeMone, 1989: Vertical velocity characteristics of oceanic convection. *J. Atmos. Sci.*, **46,** 621–640.

——, E. J. Zipser, and M. A. LeMone, 1985: Vertical motions in intense hurricanes. *J. Atmos. Sci.*, **42,** 839–856.

LaSeur, N. E., and H. F. Hawkins, 1963: An analysis of Hurricane Cleo (1958) based on data from research reconnaissance aircraft. *Mon. Wea. Rev.*, **91,** 694–709.

Lawson, R. P., 1988: The measurement of temperature from an aircraft in cloud. Ph.D. dissertation, University of Wyoming, Laramie, WY, 336 pp.

——, and W. A. Cooper, 1990: Performance of some airborne thermometers in clouds. *J. Atmos. Oceanic Technol.*, **7,** 480–494.

——, and A. R. Rodi, 1992: A new airborne thermometer for at-

Unauthenticated | Downloaded 02/22/24 05:18 AM UTC

mospheric and cloud physics research. Part I: Design and preliminary flight tests. *J. Atmos. Oceanic Technol.,* **9,** 556–574.
LeMone, M. A., 1980: On the difficulty of measuring temperature and humidity in clouds: Comments on ''Shallow convection on day 261 of GATE: Mesoscale arcs.'' *Mon. Wea. Rev.,* **108,** 1702–1707.
Lenschow, D. H., and W. T. Pennell, 1974: On the measurement of in-cloud and wet-bulb temperatures from an aircraft. *Mon. Wea. Rev.,* **102,** 447–454.
Lucas, C. E., E. J. Zipser, and M. A. LeMone, 1994: Vertical velocity in oceanic convection off tropical Australia. *J. Atmos. Sci.,* **51,** 3183–3193.
Merceret, F. J., 1982: The sensitivity of variables computed from RFC WP-3D flight data to fluctuations in the raw data inputs. NOAA Tech. Memo. ERL RFC-8, 43 pp.
——, and T. L. Schricker, 1975: A new hot-wire liquid cloud water meter. *J. Appl. Meteor.,* **14,** 319–326.
Powell, M. D., 1987: Changes in low-level kinematic and thermodynamic structure of Hurricane Alicia (1983) at landfall. *Mon. Wea. Rev.,* **115,** 75–99.
——, 1990: Boundary layer structure and dynamics in outer hurricane rainbands. Part II. Downdraft modification and mixed layer recovery. *Mon. Wea. Rev.,* **118,** 918–938.
Pruppacher, H. R., and J. D. Klett, 1997: *Microphysics of Clouds and Precipitation.* Kluwer Academic Publishers, 954 pp.
Riehl, H., 1954: *Tropical Meteorology.* McGraw Hill, 392 pp.
——, 1981: Vertical exchange of momentum and energy in the subcloud layer of Australian Hurricane Kerry (1979). *Tellus,* **33,** 105–108.
——, and J. Malkus, 1961: Some aspects of Hurricane Daisy (1958). *Tellus,* **13,** 181–213.
Rogers, R. F., S. Aberson, J. Kaplan, and S. Goldenberg, 2002: A pronounced upper-tropospheric warm anomaly encountered by the NOAA G-IV aircraft in the vicinity of deep convection. *Mon. Wea. Rev.,* **130,** 180–187.
Ryan, B. F., G. M. Barnes, and E. J. Zipser, 1992: A wide rainband in a developing tropical cyclone. *Mon. Wea. Rev.,* **120,** 431–447.
Samsury, C. E., and E. J. Zipser, 1995: Secondary wind maxima in hurricanes: Airflow and relationship to rainbands. *Mon. Wea. Rev.,* **123,** 3502–3517.
Shea, D. J., and W. M. Gray, 1973: The hurricane's inner core region. I. Symmetric and asymmetric structure. *J. Atmos. Sci.,* **30,** 1544–1564.
Sheets, R. C., 1967a: On the structure of Hurricane Janice (1958). NOAA Tech. Memo. ERL NHRL-76, 38 pp.
——, 1967b: On the structure of Hurricane Ella (1962). NOAA Tech. Memo. ERL NHRL-77, 33 pp.
——, 1968: The structure of Hurricane Dora (1964). NOAA Tech. Memo. ERL NHRL-83, 64 pp.
Simpson, R. H., 1952: Exploring eye of Typhoon ''Marge,'' 1951. *Bull. Amer. Meteor. Soc.,* **33,** 286–298.
Spyers-Duran, P. A., 1968: Comparative measurements of cloud liquid water using heated wire and cloud replicating devices. *J. Appl. Meteor.,* **7,** 674–678.
Wei, D., A. M. Blyth, and D. J. Raymond, 1998: Buoyancy of convective clouds in TOGA COARE. *J. Atmos. Sci.,* **55,** 3381–3391.
Willoughby, H. E., and M. B. Chelmow, 1982: Objective determination of hurricane tracks from aircraft observations. *Mon. Wea. Rev.,* **110,** 1298–1305.
——, J. A. Clos, and M. G. Shoribah, 1982: Concentric eyewalls, secondary wind maxima, and the evolution of the hurricane vortex. *J. Atmos. Sci.,* **39,** 395–411.
Zipser, E. J., R. J. Meitin, and M. A. LeMone, 1981: Mesoscale motion fields associated with a slowly moving GATE convective band. *J. Atmos. Sci.,* **38,** 1725–1750.

Unauthenticated | Downloaded 02/22/24 05:18 AM UTC